Electronic Supplementary Material (ESI) for Chemical Science.

Supplementary Material for: "Tuning reactivity in trimetallic dual-atom alloys: Molecular-like electronic states and ensemble effects"

Shengjie Zhang,[1] E. Charles H. Sykes,[2] Matthew M. Montemore[1]*

[1] Department of Chemical and Biomolecular Engineering, Tulane University, New Orleans, LA 70118, USA

[2] Department of Chemistry, Tufts University, Medford, MA 02155, USA

*mmontemore@tulane.edu

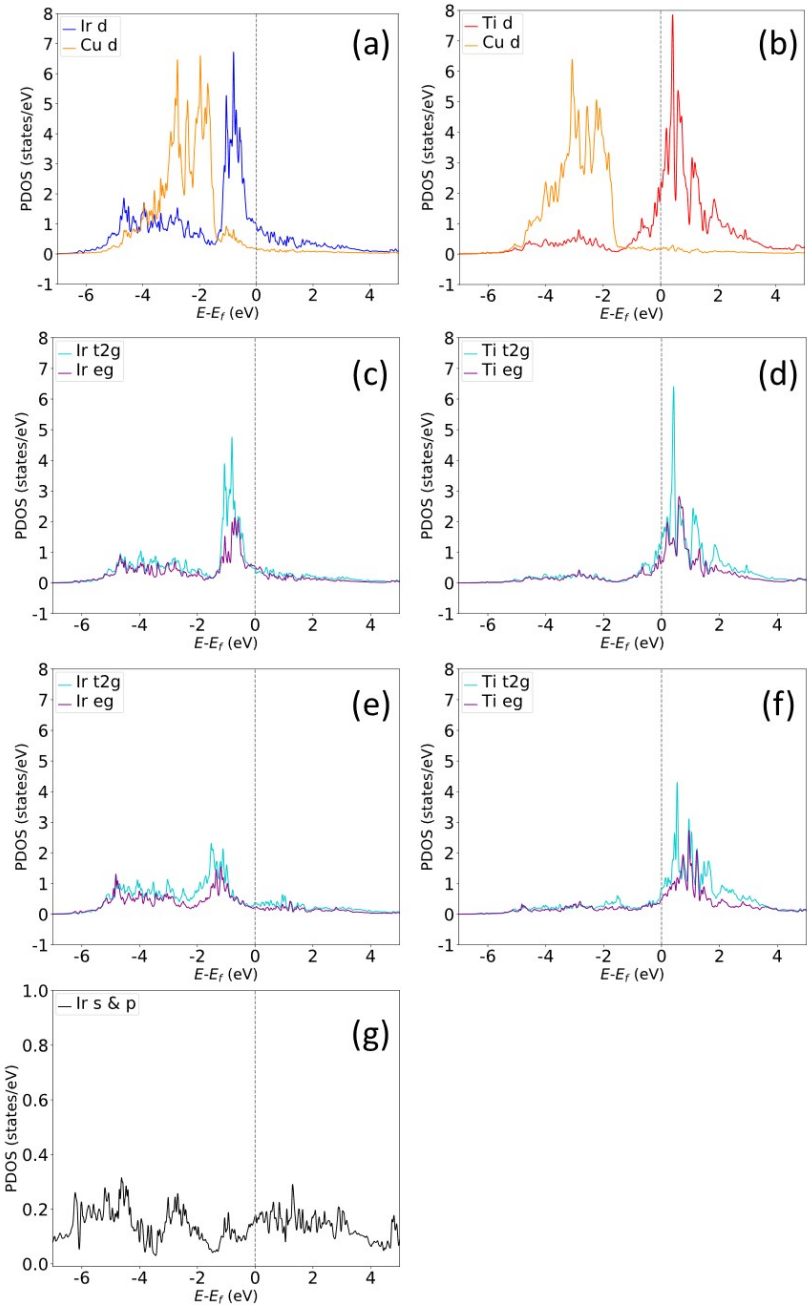

Fig. S1 (**a**) d-states of Ir and Cu in Ir_1Cu. (**b**) d-states of Ti and Cu in Ti_1Cu. (**c**), (**d**) Symmetry-resolved pDOS of Ir in Ir_1Cu and Ti in Ti_1Cu. The overlaps exhibit nearly degenerated d states, indicating very small interactions with Cu. (**e**), (**f**) Symmetry-resolved pDOS of Ir and Ti in Ir_1Ti_1Cu. Ir t_{2g}-states shift to lower energies near -2 eV and Ti t_{2g}-states shift to higher energies near 2 eV, as the Ir-Ti hybridization results in bonding and antibonding-like d-states. (**g**) s- and p-states of Ir in Ir_1Cu, which are smaller and broader than its d-states.

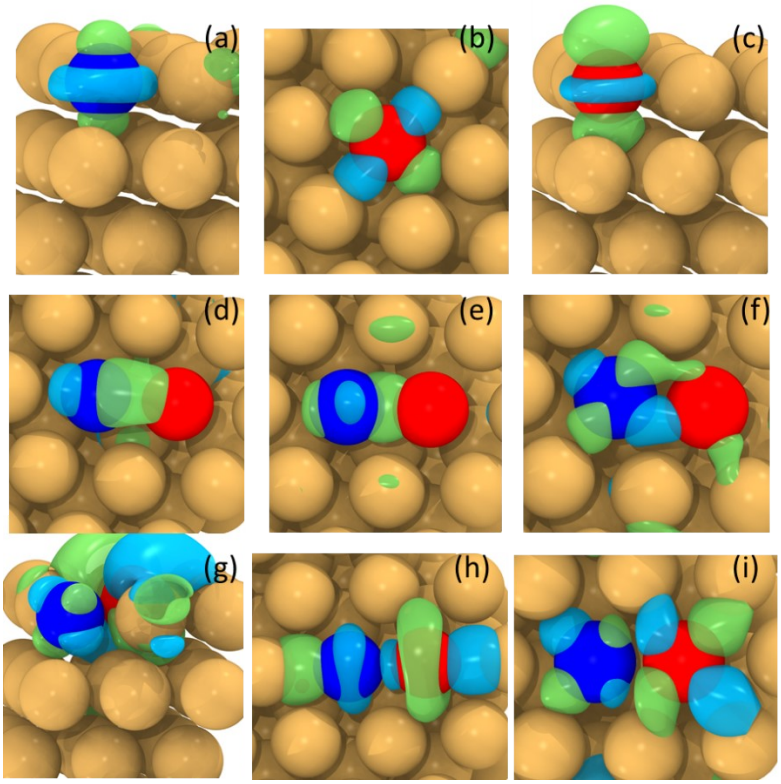

Fig. S2 Additional top views of calculated wavefunctions in Ir_1Ti_1Cu beyond those presented in Figure 1. (**a**) Ir d_{z2} in Ir_1Cu. (**b**) Ti d_{x2-y2} in Ti_1Cu. (**c**) Ti d_{z2} Ti_1Cu. (**d**) - (**f**) Ir-Ti d-d σ and π states in Ir_1Ti_1Cu. (**f**) – (**h**) Ir-Ti d-d δ*, σ* and π* states in Ir_1Ti_1Cu.

Table S1. Homodimer and heterodimer formation energies for M_1Pd_1Ag, M_1Pd_1Au, M_1Pt_1Ag, and M_1Ti_1Cu in eV.

	M_1Pd_1Ag		M_1Pd_1Au		M_1Pt_1Ag		M_1Ti_1Cu	
Dopant	Hetero-	Homo-	Hetero-	Homo-	Hetero-	Homo-	Hetero-	Homo-
Co	-0.03	-0.39	0.06	-0.18	-0.12	-0.39	-0.73	-0.35
Cr	-0.07	0.14	0.09	0.29	-0.19	0.14	0.03	0.02
Cu	0.00	0.01	0.05	0.05	-0.02	0.01	/	/
Fe	-0.07	-0.40	0.05	-0.05	-0.21	-0.40	-0.51	-0.40
Hf	-0.53	-0.13	-0.12	0.44	-0.89	-0.13	0.33	0.66
Ir	0.03	-0.20	0.14	-0.14	-0.04	-0.20	-0.83	0.08
Mn	-0.13	0.08	0.02	0.25	-0.27	0.08	-0.02	0.21
Mo	-0.17	-3.05	0.04	-2.01	-0.38	-3.05	-0.99	-2.08
Ni	0.01	-0.01	0.12	0.10	-0.05	-0.01	-0.31	0.01
Pd	0.03	0.03	0.13	0.13	0.03	0.03	-0.20	0.16
Pt	0.03	0.02	0.12	0.09	0.02	0.02	-0.38	0.25
Re	-0.19	-2.33	0.02	-1.63	-0.43	-2.33	-1.04	-1.42
Rh	0.05	0.04	0.17	0.13	0.00	0.04	-0.71	0.19
Ru	0.02	-0.81	0.13	-0.55	-0.10	-0.81	-1.15	-0.30
Sc	-0.38	0.30	-0.06	0.64	-0.66	0.30	0.47	0.82
Ta	-0.46	-1.48	-0.11	-0.22	-0.85	-1.49	-0.16	-0.45
Tc	-0.14	-3.69	0.04	-3.44	-0.33	-3.70	-1.30	-1.38
Ti	-0.30	-0.30	-0.03	0.15	-0.62	-0.30	0.07	0.07
V	-0.13	-0.64	0.07	0.15	-0.32	-0.64	-0.13	-0.58
W	-0.26	-2.53	-0.05	-1.56	-0.58	-2.54	-0.66	-1.43

Table S2. DFT energies of CO adsorption on atop site of M in M_1H ($E_{ads(SAA)}$), atop site of M in $M_1M'_1H$ ($E_{ads(DAA, M)}$), atop site of M′ ($E_{ads(DAA, M')}$) and bridge site ($E_{ads(DAA, Bri)}$) in eV. The lowest energy site for each dual-atom case are in bold. Strong electronic effects are indicated if the CO top-site adsorption energy changes by more than 0.14 eV between the SAA and DAA. Strong ensemble effects are indicated if the bridge site is the most stable site on the DAA.

	SAAs (M_1H)	Dual-atom sites ($M_1M'_1H$)				
	top CO on M ($E_{ads(SAA)}$)	top CO on M ($E_{ads(DAA, M)}$)	top CO on M' ($E_{ads(DAA, M')}$)	bridge CO ($E_{ads(DAA, Bri)}$)	Electronic effect?	Ensemble effect?
Pd_1Ag	-1.32					
$Ni_1(Pd_1)Ag$	-1.88	**-1.87**	-1.34		strong	weak
$Cr_1(Pd_1)Ag$	-1.27	-1.27	-1.34	**-1.52**	weak	strong
$Cu_1(Pd_1)Ag$	-0.92	-0.90	**-1.35**	-1.31	weak	weak
$Hf_1(Pd_1)Ag$	-1.57	-1.43	-1.16	**-1.51**	strong	strong
$Mn_1(Pd_1)Ag$	-1.19	-1.11	-1.31	**-1.39**	weak	strong
$Sc_1(Pd_1)Ag$	-1.05	-0.98	-1.25	**-1.29**	weak	strong
$Ti_1(Pd_1)Ag$	-1.51	-1.52	-1.25	**-1.60**	weak	strong
Pd_1Au	-1.20					
$Hf_1(Pd_1)Au$	-1.35	-1.29	-1.17	**-1.37**	weak	strong
$Sc_1(Pd_1)Au$	-0.94	-0.91	**-1.25**	-1.19	weak	weak
$Ti_1(Pd_1)Au$	-1.41	-1.37	-1.23	**-1.49**	weak	strong
Ti_1Cu	-1.42					
$Ru_1(Ti_1)Cu$	-2.63	**-2.26**	-1.20	/[a]	strong	weak
$Ir_1(Ti_1)Cu$	-2.52	**-2.22**	-1.29	/[a]	strong	weak
$Co_1(Ti_1)Cu$	-2.44	**-2.28**	-1.28	/[a]	strong	weak
$Rh_1(Ti_1)Cu$	-2.18	**-1.94**	-1.42	/[a]	strong	weak
$Fe_1(Ti_1)Cu$	-2.02	**-2.33**	/[a]	/[a]	strong	weak
$Ni_1(Ti_1)Cu$	-1.80	**-1.72**	-1.37	-1.72	weak	weak
$Pt_1(Ti_1)Cu$	-1.59	-1.40	**-1.50**	-1.39	strong	weak
$Mn_1(Ti_1)Cu$	-1.42	**-2.14**	-1.28	/[a]	strong	weak
$Pd_1(Ti_1)Cu$	-1.29	-1.19	**-1.51**	-1.47	weak	weak

[a] CO transfers to the lowest energy site

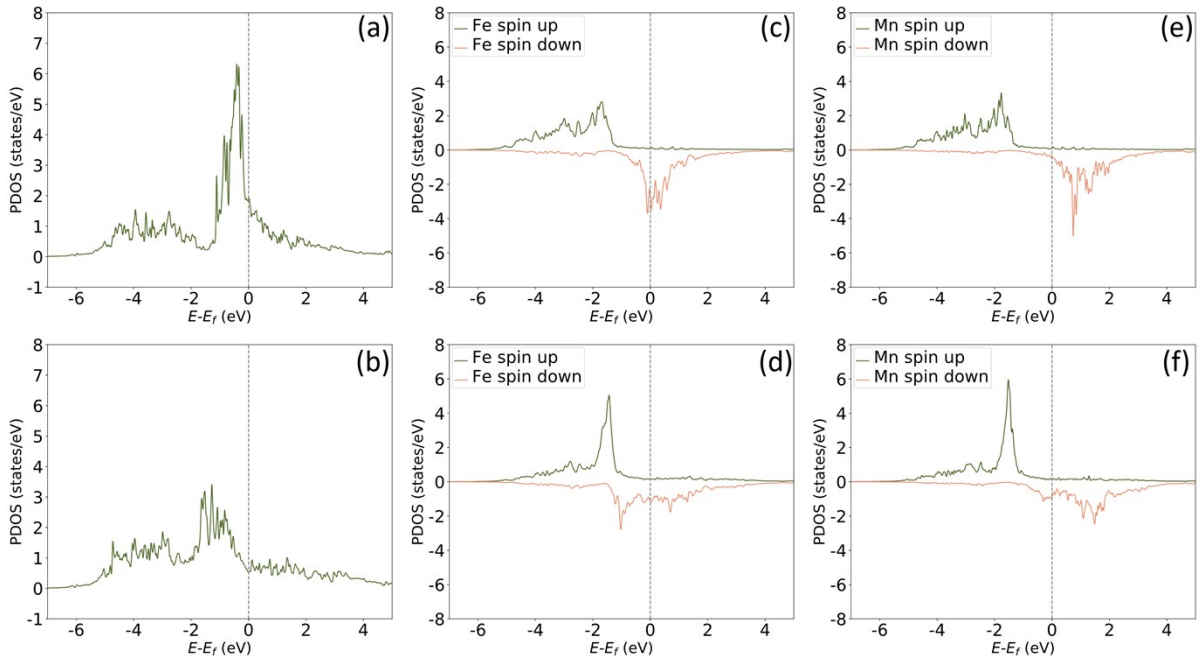

Fig. S3 pDOS of d-states of Ru, Fe, and Mn in (**a**) Ru_1Cu; (**b**) Ru_1Ti_1Cu; (**c**) Fe_1Cu; (**d**) Fe_1Ti_1Cu; (**e**) Mn_1Cu and (**f**) Mn_1Ti_1Cu. The shape and d-band center are significantly changed from SAAs (**a**, **c**, **e**) to dual-atom alloy sites (**b**, **d**, **f**), showing significant electronic effects.

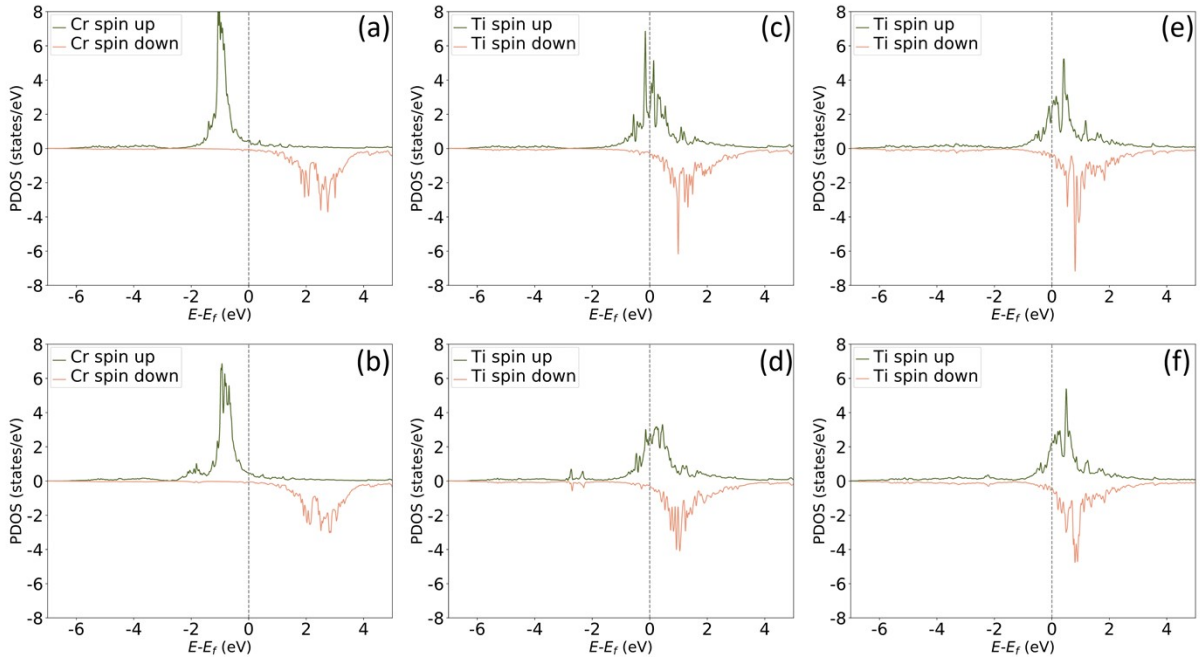

Fig. S4 pDOS of d-states of Cr and Ti in (**a**) Cr_1Ag; (**b**) Cr_1Pd_1Ag; (**c**) Ti_1Ag; (**d**) Ti_1Pd_1Ag; (**e**) Ti_1Au and (**f**) Ti_1Pd_1Au. The shape and d-band center are almost identical between SAAs (**a**, **c**, **e**) and dual-atom alloy sites (**b**, **d**, **f**), showing negligible electronic effects.